SYNTHESIS OF LITHIUM ORTHOSILICATE BY POLYMER PRECURSOR ROUTE

SUBMITTED BY

SATYA PRAKASH SAHOO

111CR0552

A THESIS SUBMITTED IN PARTIAL FULFILLMENT OF THE REQIREMENTS FOR THE

DEGREE OF BACHELOR OF TECHNOLOGY

Supervised By

PROF. S.K.BEHERA

DEPARTMENT OF CERAMIC ENGINEERING

NATIONAL INSTITUTE OF TECHNOLOGY ROURKELA

CERTIFICATE

This is to certify that the thesis entitled **"Synthesis of Lithium Orthosilicate by Polymer Precursor Route"** is submitted by **Mr. Satya Prakash Sahoo** for the degree for Bachelor of Technology (B.Tech) in Ceramic Engineering to National Institute of Technology, Rourkela, which is a evidence of research work carried out by him under my guidance. In our opinion his thesis is worthy of consideration for the award of degree of Bachelor of Technology in accordance with the regulations of the institute. The results present in this thesis have not been submitted to any other university or institute for the award of a Degree.

PROF S.K BEHERA

DEPARTMENT OF CERAMIC ENGINEERING

NATIONAL INSTITUTE OF TECHNOLOGY

ROURKELA

Acknowledgements

I would like to express my deep gratitude to my project supervisor, Prof. S.K. Behera, Department of Ceramic Engineering, NIT Rourkela for his valuable advice and guidance for completion of the project work.

I express my sincere thanks to Prof. Swadesh Pratihar, Head of Ceramic Engineering Department for providing me all the departmental facilities required for the completion of the thesis. I am also thankful to all other faculty members of Ceramic Engineering Department, NIT Rourkela for their invaluable advice, constant help, encouragement, inspiration and blessings.

I also acknowledge the help and cooperation of Phd scholar Abhisek bhai for helping me to complete my project. Last but not the least I also acknowledge gratefully the help and cooperation extended by all the non-teaching staffs of the department.

SATYA PRAKASH SAHOO

CONTENTS

List of Figures

Chapter-1

INTRODUCTION

1.1 Lithium based Ceramics- Uses and Applications

Lithium based ceramics have applications in various fields which have been described as follows:

1.1.1 Tritium breeders in thermonuclear fusion reactors

Now a days the energy requirement has increased in every aspect of daily life. But, we are still dependent on a number of non-renewable resources like Natural gas and Coal which pollute the environment by giving out greenhouse gases. Some studies have also shown that all the fossil fuel will be depleted within a few decades. So we require some alternative sources of energy which can be used by us and our generations to come in the future.

Nuclear energy can be used in the future as an alternative to non-renewable sources of energy. Today all the nuclear energy that we use is derived from nuclear fission, where splitting of a heavy nucleus such as U-235 occurs in to two lighter nuclei with release of large amount of energy.

On the contrary fission technology results in a number of problems related to safety issues and radioactive waste generation. In response to safety issues, energy harvesting through fusion process is much safer than energy production from fission process.

Nuclear fusion is the union of two light nuclei that results in a heavier nuclei plus energy. It can be seen from figure 1 that fusion reaction releases much higher energy than fission reaction. Also, the radioactive waste from fusion devices is very less compared to the waste generated in fission reaction.

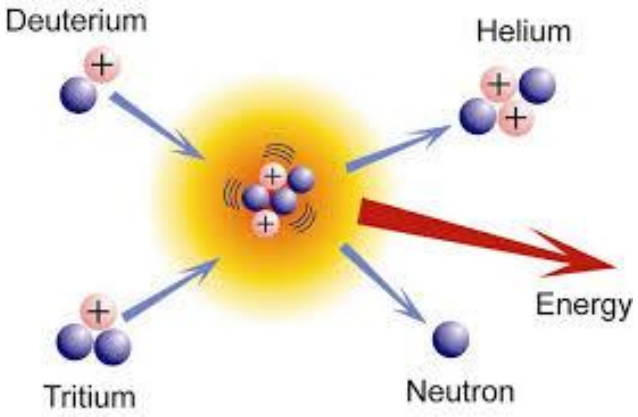

$$^{2}_{1}D + ^{3}_{1}T \rightarrow ^{4}_{2}He(3.5MeV) + n^{0}(14.1MeV)$$

Fig. 1.1 Fusion reaction of deuterium and tritium
[http://newenergyandfuel.com/http:/newenergyandfuel/com/2011/11/30/more-fantastic-fusion-than-rossi%E2%80%99s-e-cat/]

The Deuterium-Tritium **(D-T)** reaction produces energetic neutrons which is the main reason for the production of energy by the nuclear reactors. In a fusion reactor the fuel amount used is very less compared with the quantity required in tones to produce the same amount of energy by fission reaction. And the output is also harm-less inert gas Helium. For the D-T reaction to occur the source of deuterium is the sea water, which can be extracted at very low cost. But tritium doesn't occur naturally on earth, but one can extract it by using lithium based ceramics. There are many lithium based ceramics that can be used for tritium breeding for the fusion reaction [1]-[3].

Among various lithium based ceramics lithium orthosilicate (Li_4SiO_4) is considered as promising solid breeder material in the tritium breeding blanket of thermonuclear fusion reactors because of high Li-density, high thermal conductivity and prominent tritium release rate at low temperatures between 300^{o}C and 500^{o}C.

1.1.2 CO_2 adsorbents

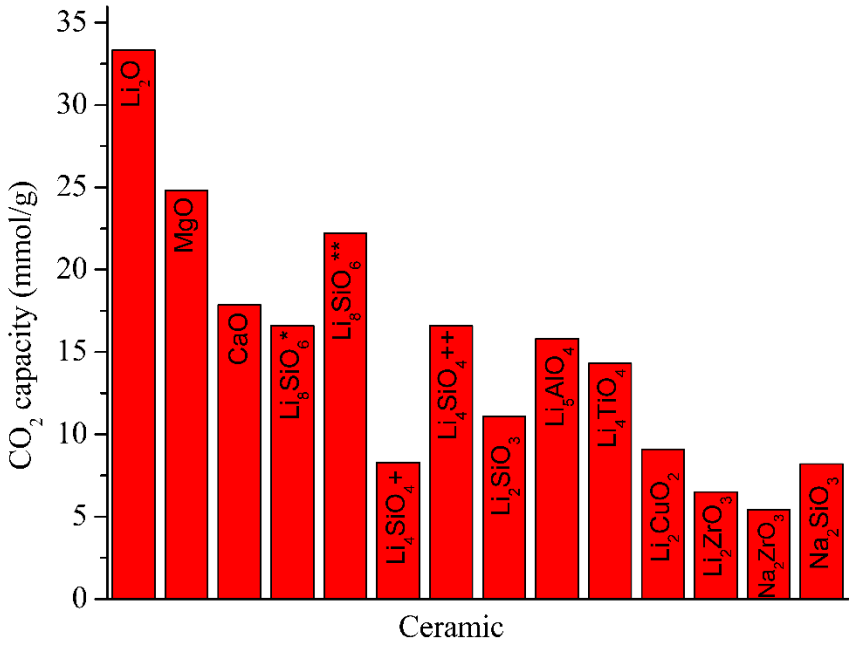

Fig 1.2 Theoretical CO_2 capture capacities for different alkaline and alkaline-earth ceramics.

Now a days fossil fuels are burnt to produce energy which results in the emission of large amount of carbon dioxide (CO_2) into the atmosphere creating environmental problems like global warming. This can have a detrimental effect on our future generations to come.

So there is a need to develop alternative sources which can save energy. This can be done by reducing the amount of CO_2 emissions in to the atmosphere. A large number of compounds have

been proposed having good capacity for absorbing CO_2 from the atmosphere as shown in figure 1.2. Lithium based ceramics are candidate materials for the high temperature absorption and removal of CO_2 that include lithium ferrite, lithium nickelite, lithium titanate, lithium metasilicate and lithium orthosilicate. Amongst these oxides, Li_4SiO_4 was found to possess adequate capacity to absorb CO_2 [4].

1.1.3 Cathode materials for Li-ion Battery

(a) (b)

Fig 1.3 (a) Lithium-ion batteries have become the dominant rechargeable battery chemistry for consumer electronics devices, (b) An example of a Li-ion battery (used on the Nokia 3310 mobile phone)

A lithium-ion battery is a member of a family of rechargeable battery types in which lithium ions move from the negative electrode to the positive electrode during discharge and back during charging. The electrolyte, which allows for ionic movement, and the two electrodes are the constituent components of a lithium-ion cell.

Lithium ion batteries provide higher energy density compared to other rechargeable battery systems such as lead acid, nickel cadmium and nickel metal hydride batteries. The higher volumetric and gravimetric energy density of Lithium ion cells are due to higher cell voltages achievable because of non-aqueous electrolytes which allow a wider temperature of operation. Lithium-ion is a low maintenance battery. In addition, the self-discharge is less than half compared to nickel-cadmium, making lithium-ion well suited for modern fuel gauge applications. Lithium-ion cells cause little harm when disposed. It has relatively low self-discharge which is less than half that of nickel-based

batteries. Various lithium based materials are utilized for the cathode material in Li-ion battery [5][6].

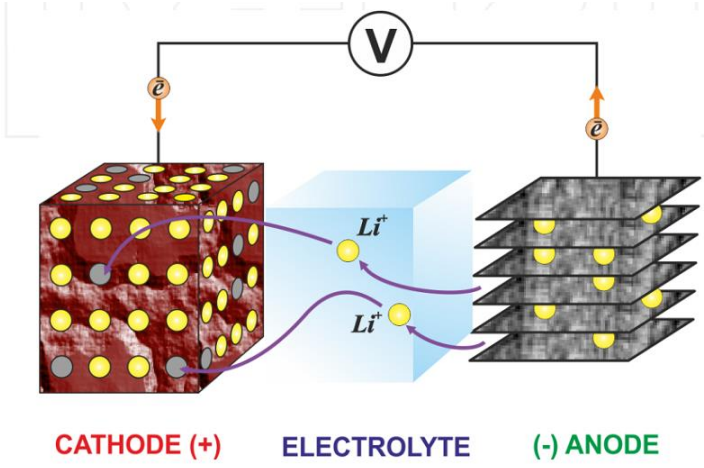

Fig 1.4 Working mechanism of Li-ion batteries (discharge cycle)

Among them lithium transition-metal orthosilicates have been characterized as potential cathode materials for use in Li-ion batteries by some researchers. These orthosilicates are different from lithium transition-metal phosphates which only have one Li ion per formula unit. Li_2MSiO_4 (M=Fe,Co,Mn) with two Li ions per formula unit ($M^{2+} \rightarrow M^{4+}$) could have a theoretical capacity that is >300 mA h g^{-1} . Thus theoretical capacity and excellent safety performance of Li_2MSiO_4 allows it to be used in the development of Li-ion batteries [7] [8].

Apart from the above major applications of lithium orthosilicate in batteries, as CO_2 absorbents and breeder materials, lithium orthosilicate also finds use in glass ceramics, concrete hardener etc. Thus, it could be seen that Lithium orthosilicate has wide applications. Various methods have been discussed for synthesis which is described in detail in the literature review.

1.2 Literature Review on synthesis of lithium orthosilicate

Researchers have used various processing techniques like solid state mixing method, urea combustion method, water based sol-gel method for the preparation of Li_4SiO_4. Source of silica is important for synthesis of Li_4SiO_4. Generally quartz powder, silicic acid, amorphous silica, fumed silica and TEOS are used as silica source.

In a study *Vollath et al* [9], [10] used amorphous silica as silica source for large scale production of Li_4SiO_4. A suspension technique was used in which silica was suspended in methanol. After wetting silica, LiOH was added for the preparation of Li_4SiO_4.In another study, *vollath et al*[11] synthesized Li_4SiO_4, along with Li_2SiO_3 and Li_6SiO_5 by spray-drying of the alcoholic suspensions followed by calcination of the residue and grinding thereafter.

Kaukis et al [12] synthesized Li_4SiO_4 by thermochemical methods using SiO_2 and Li_2CO_3 as the precursors for Si and Li respectively. *Tao tang et al* [13] prepared Li_4SiO_4 through conventional solid state method by using amorphous silica and Li_2CO_3.

Cruz et al [14] used silicic acid as the silica source for synthesizing Li_4SiO_4 along with Lithium hydroxide and Urea. *Pfeifer et al* [15] used amorphous silica gel and TEOS as the source of silica for the synthesis of Li_4SiO_4. Three different methods were followed namely solid state, precipitation and sol-gel methods for the synthesis of Li_4SiO_4. Fumed silica with very high specific surface area (~350m^2/gm) was used by *Chang et al* [16] for preparing of Li_4SiO_4. Two different sources of lithium were used *viz* lithium nitrate and lithium hydroxide.

Wu et al [17] utilized aerosil silica as the silica source for the synthesis of Li_4SiO_4 along with hydrated LiOH. They followed water based sol-gel method in which citric acid is used as a chelating agent. Recently *Choudhary et al[18]* also synthesized lithium orthosilicate by combustion technique using RHA as the source of silica and lithium nitrate. They also used citric acid as the source of fuel and chelating agent.

It can be concluded from literature review that various authors have used different sources of silica for the synthesis of lithium orthosilicate. The source and purity of silica plays a major role in the phase formation of lithium orthosilicate. Various authors have employed solid state synthesis for the synthesis which requires high temperature (>1200^oC) that results in larger grain size. Sol-gel synthesis also requires costly precursors like TEOS for the preparation of lithium silicate ceramics. Combustion route can also produce phase pure lithium silicate but the addition of fuel and then removal of carbonaceous matter. In our work we present a novel approach for synthesizing lithium orthosilicate from a polymer precursor route. The advantage, applications and various properties of polymer derived ceramics have been outlined below.

1.3 Polymer Derived Ceramics: Advantages and Application [18]

The formation of ceramic materials via the polymer route (*polymer-derived ceramics*) is an alternative to the conventional ceramic processing involving powders. Starting with a pre-ceramic polymer compound (primarily Si-based, such as polysiloxanes, polysilazanes), a controlled thermal decomposition yields amorphous or crystalline ceramic materials.

Advantages:

a) In PDCs near-net shapes can be produced which is not possible by other conventional techniques.
b) PDCs are additive-free ceramic materials possessing excellent oxidation and creep resistance up to exceptionally high temperatures; whereas powder routes require sintering additives.
c) The relatively low synthesis temperature (thus lower energy consumption) of 1100^{o}C –1300^{o}C makes the production of PDCs an economical interest.
d) Ternary compositions like SiCN, SiCO cannot be synthesized through other techniques other than the molecular approach (the same approach for producing PDCs).

Some of the processing advantages (i.e., use of preceramic polymers over molecular precursors, e.g. sol-gel) involve

a) Preceramic polymers do not have any drying problems, hence bulk components can be fabricated easily
b) Do not require flammable solvents
c) Can be pressed in molten state
d) Do not require special handling procedures, especially in case of polysiloxanes
e) Machining before ceramization avoids problems connected to tool wear and brittle fracture upon finishing of component
f) During joining, precursor effectively binds together parts at low temperature, therefore making handling before heat treatment simpler

Properties:

a) High chemical durability (oxidation resistance)
b) High creep resistance
c) Semiconducting behaviour
d) Better thermomechanical properties

Properties of PDCs in detail

a) Electrical properties

The room temperature dc conductivity of PDCs varies up to 15 orders of magnitude (typically in the range 10^{-10}–10^{-8} to 1 $(\Omega.cm)^{-1}$) depending on the polymeric precursor, composition, pyrolysis temperature, and atmosphere. For low pyrolysis temperature ($T_{pyrolysis}$) ~<600^0C, PDCs behave as insulators while in case of amorphous PDCs, obtained at $T_{pyrolysis}$ ~>800^0C, conductivity increases with temperature at which it is measured, showing typical semiconducting behaviour. The conductivity of PDCs can also be changed by adding filler particles to the preceramic matrix.

Nature of the conduction mechanism in amorphous PDCs is obtained from temperature and frequency dependences of the corresponding conductivities. It was found experimentally that conductivity is due to the hopping of carriers between localized states in the mobility gap.

b) Magnetic properties

PDCs that contain iron, exhibit magnetic properties. An elegant approach to produce PDCs with magnetic functionalities comprises the incorporation of the metallic iron atoms into the backbone of the polymeric precursor.

c) Optical properties

Since PDCs are generally black and their optical properties have received little attention. The reason for the black colour of PDC has been generally ascribed to the presence of sp^2 C atoms, which form absorbing graphene layers in the ceramic structure.

d) Chemical properties

- *Oxidation resistance:* PDCs pyrolyzed at a temperature high enough to completely remove the hydrogen from the system, parabolic oxidation rates are observed. These studies showed the formation of a dense and continuous oxide layer (without bubbles or cracks), with a sharp oxide/ceramic interface. SiCO and SiCNO PDCs possess a negative enthalpy to their relative crystalline constituents in agreement with the proposed lower activity (<1) of free carbon.
- *Chemical durability:* The SiCO network exhibits greater durability than the pure silica glass, SiO_2, in both basic and acidic media because of the character of the bonding (Si–C bonds are less prone to nucleophilic attack) and a higher degree of compositional disorder and network cross-linking carbon (either bonded to Si atoms or present as a ‘‘free’’-carbon

phase, impedes reactant transport locally). If the SiCO is pyrolyzed at high-temperatures ($T \geq 1200^0 C$) it undergoes a phase separation into SiO_2-based, SiC and carbon regions and the chemical durability decreases since the SiO_2 species can be extracted.

e) Mechanical properties

PDCs have open structures, thus leading to low density values. The elastic modulus and density increase with the pyrolysis temperature due the increased network connectivity realized by stripping the hydrogen present in residual C–H bonds. The Poisson's ratio, ν, has been reported for a limited number of PDCs and the values are generally quite low. A Poisson's ratio of 0.11 is the lowest reported value for glasses and polycrystalline ceramics and can be explained by the low atomic packing density and high crosslinking degree of silicon oxycarbide glasses. Hardness increases by increasing (i) the pyrolysis temperature and (ii) the amount of C inserted into the silica amorphous network. By increasing the pyrolysis temperature in both SiCO and SiCN systems, the dehydrogenation of the amorphous ceramic leads to a more interconnected network, which in turn, results into a lower contribution of the volume densification and a higher contribution of the shear deformation. Fracture toughness, K_{IC}, values between 0.56 and ≈3 $MPa.m^{1/2}$ have been reported. Si-based PDCs exhibit a remarkable creep resistance. Viscosity of amorphous PDC is two to three orders of magnitude higher than vitreous silica and the highest measured value for a glass at high temperatures.

Applications:

PDCs are applied in fields of

a) High temperature resistant materials (energy materials, automotive, aerospace, etc.)
b) Hard materials
c) Chemical engineering (catalyst support, food and biotech, etc.)
d) Functional material

Some of the applications include

a) As ceramic fibers. PDCs as ceramic fibers offer a decrease in oxygen contamination from 15% to <0.5 wt%, with improvement in high temperature stability and better mechanical properties.
b) Ceramic-matrix composites manufactured from preceramic polymers have an interesting novel application as brake components for high performance motor bikes, with potential for use in automobiles, trucks, trains, and airplanes. They offer excellent cold friction, are unaffected by

moisture, and are resistant to high-temperature performance fade; thus contributing to decreasing weight, improving stopping power and improving vehicle efficiency.

c) Preceramic polymers can produce polymer-derived porous ceramics whose applications include impact absorption, thermal protection, adsorption, gas separation, and 3D reinforcement for metal-matrix composites.

d) Preceramic layers processed at low temperature (ambient to $<100^0$C) are used to coat large surfaces thus forming a clear, transparent, protective and permanent coating that is essentially hydrophobic and oleophobic in nature, i.e., do not allow inks, permanent markers, spray paints, stickers and dirt, tree sap and other stains to stick to the surface, while protecting the surface from weathering, corrosion, and oxidation.

e) PDC nano-, and microsystems have found applications in photonics and fluidic devices, and as components for electrical heating (micro igniters or glow plugs), microparts and actuators.

f) The tunable electrical properties, high piezoresistivity, together with the micro fabrication capability and excellent high-temperature thermal and mechanical properties, make the polymer-derived Si–C–N and Si–O–C excellent candidate materials for high-temperature sensors and ceramic MEMS for high temperature/ corrosive-environment applications, micro glow plugs and electrode materials for Li-ion batteries.

g) Due to *in situ* conversion to ceramic during service, polymer-based mixture in the polymeric state is used as sealant for repair of small cracks and gouges that can result from damage to the reinforced carbon-carbon composite of the Space Shuttle's wing leading edge or nose caps.

1.4 OBJECTIVE OF THE PROJECT

My objective in this project is to synthesize phase pure lithium orthosilicate by using a novel polymer precursor route and simultaneously compare the results with lithium orthosilicate prepared by conventional solid state method. Source of silica is very important for the formation of lithium orthosilicate. For our work, the objective can be broadly highlighted as follows:

1. To study the effect of different sources of silica on the phase formation behaviour of lithium orthosilicate.
2. To compare the properties (thermal and microstructural) of lithium orthosilicate derived from polymer route and conventional solid state route.
3. To study the densification behaviour of polymer derived lithium orthosilicate and solid state synthesized lithium orthosilicate.
4. To study the effect of non-stoichiometric amount of silica on lithium sublimation.

Approach for attaining the above objectives has been described as follows:

- We utilised two different source of silica *viz.* silicone containing polymer i.e. polymethylsilsesquioxane and microfine silica.
- With the same preceramic polymer precursor, three different batches were prepared taking different amount (based on ceramic yield) of preceramic polymer i.e silica rich, stoichiometric silica and silica lean keeping source of lithium constant in all batches.

CHAPTER 2

EXPERIMENTAL PROCEDURE

.

2.1 Raw material properties

Polymethyl silsesquioxane (Silres)

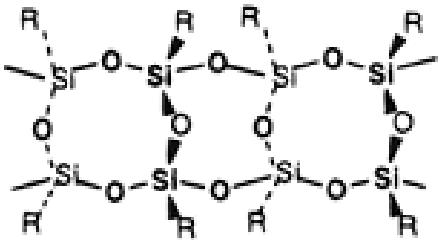

Fig 2.1 Simplified representation of Ladder type structure of silsesquioxane

The term silsesquioxanes refers to all structures with the empirical formula $RSiO_{3/2}$ where R is hydrogen or any alkyl, alkylene, aryl, arylene, or organo-functional derivative of alkyl, alkylene, aryl, or arylene groups. The structures of silsesquioxanes have been reported as random structure, ladder structure, cage structures, and partial cage structure. In this project solid silicone powder Polymethylsilsesquioxane (Silres, Wacker Chemie AG, Burghausen, Germany) was taken as the source of preceramic polymer for the preparation of lithium orthosilicate. The structure of polymethylsilsesquioxanes is ladder type as shown in fig 2.1.

The initial thermal decomposition temperature of polymethylsiloxane is somewhat lower than that of polyphenylsilsesquioxane. Polymethylsilsesquioxanes are simply described to have ladder structures based on their IR spectra. Polymethylsilsesquioxane is characterized by its low weight loss at high temperatures of 800^{o}C, although the initial decomposition temperature is somewhat lower than that of polyphenylsilsesquioxane. Polymethylsilsesquioxane is also used as a binder for ceramics.

Isopropyl Alcohol (IPA)

Iso-propyl alcohol (Emplura, Merck chemicals, India) was also used as a solvent for dissolving the preceramic polymer. Isopropyl alcohol is a chemical compound with the molecular formula C_3H_8O or C_3H_7OH or $CH_3CHOHCH_3$. It is a colorless, flammable chemical compound with a strong odor.

Lithium carbonate (Li_2CO_3)

Lithium carbonate (ACS, 99% purity, Merck chemicals, Germany) was used as the source of lithium. This white salt is widely used in the processing of metal oxides.

Triethanolamine (TEA)

Triethanolamine (98% pure, Lobachemie, India) was used as a crosslinking agent to develop more network in the side chains of polymer.

2.2 Preparation of Lithium Orthosilicate powder and Subsequent Characterizations

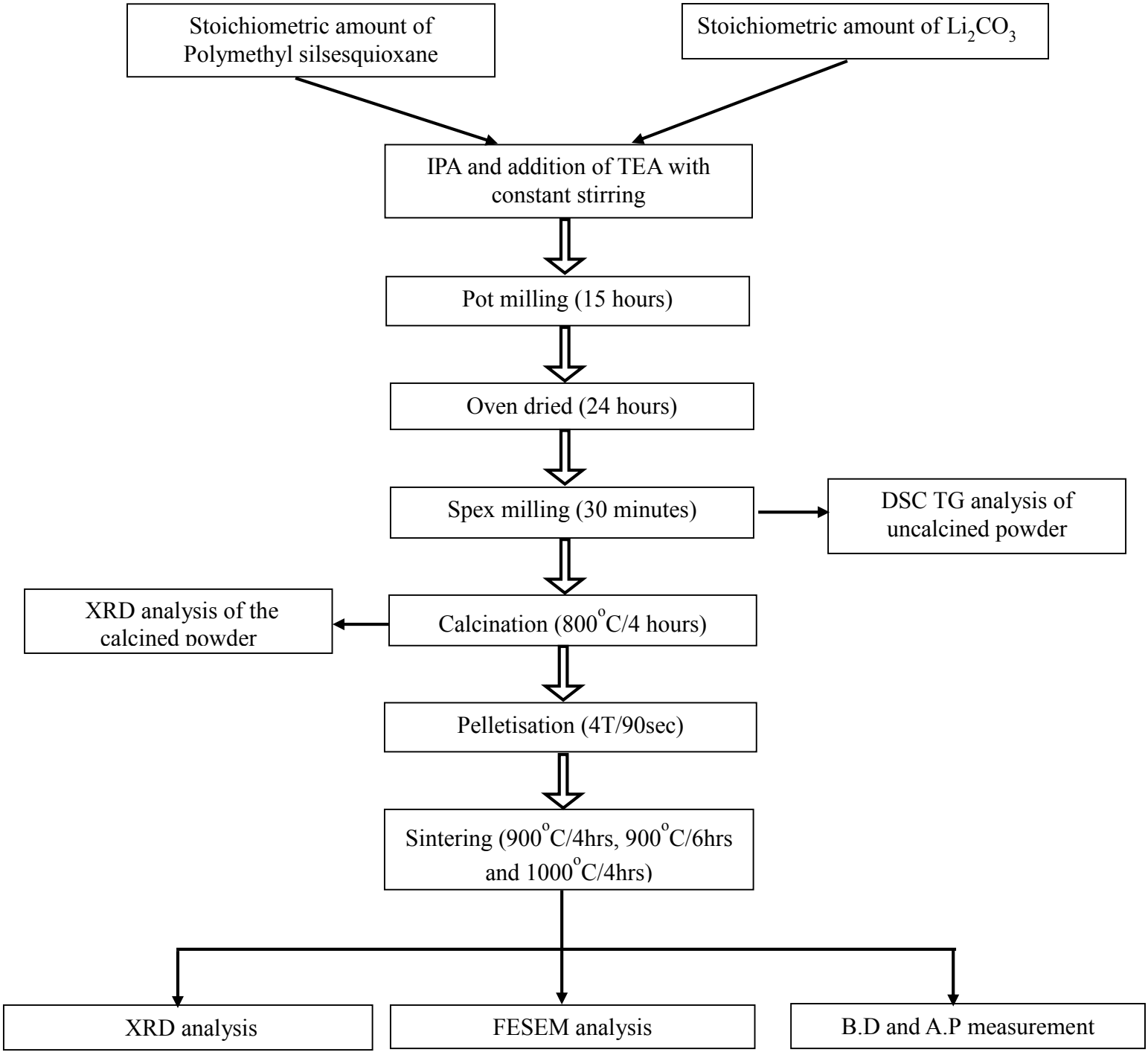

Fig 2.2 Flow chart of Lithium Orthosilicate preparation and characterizations

The flowchart for the preparation of lithium orthosilicate have been presented in figure 2.1.Stoichiometric amounts of preceramic polymer and lithium carbonate were taken to prepare silica lean (considering 82% silica yield from the polymer), silica rich (taking 78% silica yield from the polymer) and stoichiometric silica (considering 80% silica yield from the polymer) batches. Stoichiometric amounts of microfine silica and lithium carbonate were also taken to prepare another batch for the sake of comparison. So over all four batches were prepared.

- 25 ml of IPA was taken in a polypropylene bottle and thereafter polymethylsilsesquioxane was added to it. After getting a clear solution $Li_2CO_3$was added. The crosslinking agent i.e. TEA was then added to the solution. The mixture was then well stirred on a magnetic hot plate for maintaining the consistency of the solution for about half an hour. For batch prepared with microfine silica no TEA was added to the mixture of Li_2CO_3 and microfine silica. Pot milling of the slurry was carried out for about 15hrs in which zirconia balls were taken as the grinding media.
- The slurry of all the four batches was carefully taken out on a petridish and then kept under the IR lamp for about 15 minutes to remove the excess solvent. Thereafter they were oven dried for about 24 hours.
- After drying the obtained powders were kept for crosslinking in a muffle furnace at 350^{o}C for a dwelling time of 2 hours.
- The crosslinked powders for all the batches were then SPEX milled for 20 minutes for uniform particle size.
- The uncalcined powders for all the four batches were then given for DSC TG analysis.
- The powders were then calcined at 800 ^{o}C for 4 hours for the phase formation of lithium orthosilicate. XRD analysis of the calcined powder (800 ^{o}C/ 4hrs) for all the four batches was done.
- The calcined powders were then ground and sufficient amount of binder was added. The binder mixed powders were then uniaxially pressed at 4 tonn with a dwelling time for 90 sec.
- The pressed pellets were sintered at 900 ^{o}C for 4 hours,6 hours and 1000 ^{o}C for 4 hours.
- XRD analysis of the sintered specimen at 1000 ^{o}C/ 4hr was done.SEM analysis of 900 ^{o}C/4hr, 900 ^{o}C/6hr and 1000 ^{o}C/4hr samples was also done.
- Bulk density and apparent porosity of all the samples was found out.

Characterizations

2.2 Thermal Analysis

The powders were characterized by differential scanning calorimeter (DSC) and thermo gravimetric analysis (TGA) by using NETZSCH STA (Model No 409C). DSC is a recent technique which was developed for quantitative calorimetric measurements. The signal from the differential scanning calorimeter is regarded as proportional to the difference in thermal power between the sample and reference, $d\Delta q/dt$. Differential scanning calorimeters uses a crucible to contain the sample. The diameter of the crucibles used is generally 5-6mm which are made of alumina. Thermal analysis is done to determine the chemical kinetics, enthalpy transitions and transformation. When a material undergoes physical or chemical change it absorbs or releases thermal energy. The temperature difference between the sample w.r.t to the reference inert material during heating or cooling is plotted in a DSC curve. Exothermic or endothermic changes are shown in opposite directions of the baseline. The heating rate was maintained at 10^{o}C/min for all the batches and all the measurement was carried in oxidative atmosphere to replicate the actual experimental conditions.

Similarly TGA is an analytical technique in which the mass change of a substance is measured as a function of temperature when the substance is subjected to a controlled temperature programme. The temperature programme must be taken to include holding the sample at a constant temperature, when the mass change is measured against time. Mass loss is only seen in a process occurs when a volatile component is lost. There are also reactions where there is no mass loss. When materials are heated, they lose weight due to drying, or from chemical reactions that liberate gasses. The results may be reported directly as mass of the sample varying with temperature or time, i.e. as m versus T. Thus a mass loss appears as a downwards curve.

2.3 X ray diffraction

Phase formation of as burnt and calcined powder samples was studied by the powder X-ray diffraction performed using a Philip's Diffractometer (model: PW-1830, Philips, Netherlands) using Cu K_{α} radiation. From this technique we can get a number of informations like crystal structure, crystalinity of the material, crystallite size, chemical analysis etc. The phases present have been identified with the search match facility available with Philips X'pert high score software. A powdered sample was packed on a sample stage so that it can be scanned by the X-ray. The

diffracted X-rays were detected by an electronic detector placed on the other side of the sample. To get the diffracted beams the sample was rotated through different Bragg's angles. After scan of the sample, the X-ray intensity (counts/sec) (Y axes) was plotted against the angle theta (2θ) (X-axes). The angle (2θ) for each diffraction peak was then converted to d-spacing, using the Bragg's law;

$$\mathbf{n\lambda = 2d\ Sin\theta}$$

where λ = wave length of x-ray , n = order of diffraction, d= interplanar spacing and θ is the bragg's angle. All the XRD were done with a 2θ scanning range = 15-60^{o} .

2.4 Microstructural Analysis

In the Field Emission Scanning Electron Microscopy (FESEM), a source of electrons is focused (in vacuum) into a fine probe that is restored over the surface of the specimen. As the electrons penetrate the surface, a large number of interactions occur which can result in the emission of electrons or photons from (or through) the surface. A reasonable fraction of the electrons emitted can be collected by appropriate detectors, and the output can be used to modulate the brightness of a cathode ray tube (CRT) whose x- and y inputs are driven in synchronism with the x-y voltages restoring the electron beam. In this way an image is produced on the CRT; every point that the beam strikes on the sample is mapped directly onto a corresponding point on the screen. Fired samples and the fractured surface were cleaned in acetone and dried at 100^{o}C for 24hr for SEM imaging. Some sample surfaces were polished on fine emery paper; the samples were thermally etched at 50^{o}C less than the sintering temperature. Powder samples were dispersed in water medium in ultrasonic vibrator (Oscar, Sonopros PR-1000MP). One drop was put on a glass plate and dried under IR lamp for 4 hr prior to the SEM imaging.

2.5 Bulk Density and Apparent Porosity

Bulk density and apparent porosity of the sintered specimens were determined by Archimedes principle. Sintered samples were weighted in dry state. Samples were immersed in kerosene and kept under a vacuum desiccators for 4 hrs to ensure that kerosene filled up the open pores completely. Then, soaked and suspended weights were measured. The apparent porosity and bulk density were calculated as follows:

B.D (Bulk Density) = $\frac{W_d}{W_s - W_a}$ **A.P** (Apparent Porosity) = $\frac{W_s - W_d}{W_s - W_a}$

W_d =Dry weight of the sample, W_s = Soaked weight of the sample, W_a =Suspended weight of the sample

Universal code names for different batch compositions

Sl. No.	Sample Description	Sample Codes	Amount of polymethylsilsesquioxane per 10gm batch (gm)
1.	Stiochiometric amount of lithium carbonate and microfine silica	MSLC	5.01
2.	Amount of polymer) and lithium carbonate – **Silica lean**	78LC	6.42
3.	Amount of polymer and lithium carbonate **–** **Stoichiometric Silica**	80LC	6.26
4.	Amount of polymer and lithium carbonate – **Silica lean**	82LC	6.11

CHAPTER-3

RESULTS AND DISCUSSION

3.1 DSC TG Analysis of raw materials and various uncalcined powders of different batches

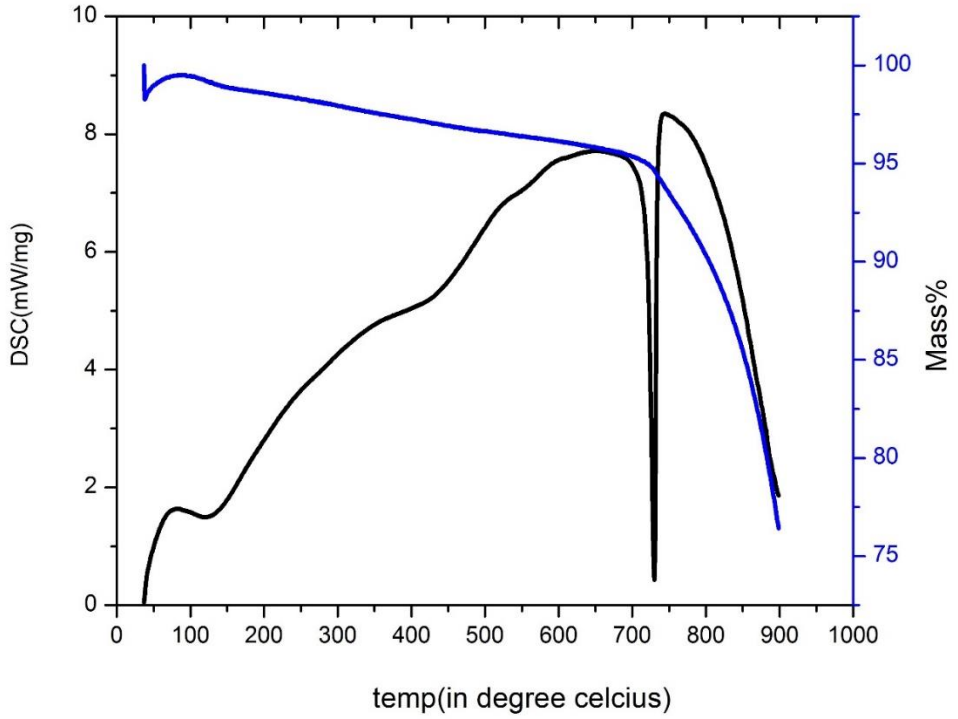

FIG 3.1 DSC TG graph of lithium carbonate (Li_2CO_3)

FIG 3.1 shows the DSC TG graph of lithium carbonate measured upto 900^oC. A small weight loss of about 5 % can be observed at 100^oC which is due to the loss of physically adsorbed water. The weight loss is also accompanied by a small endothermic peak between 100^oC - 150^0C. From the DSC curve we could observe that a sharp endothermic peak appears at 730^oC .This peak arises due to the decomposition of Li_2CO_3 into Li_2O and CO_2. [19]Simultaneously from the TG Curve, a weight loss of about 18% was also observed due to the decomposition of lithium carbonate. An overall weight loss of about 25% can be observed from room temperature till 900^oC.

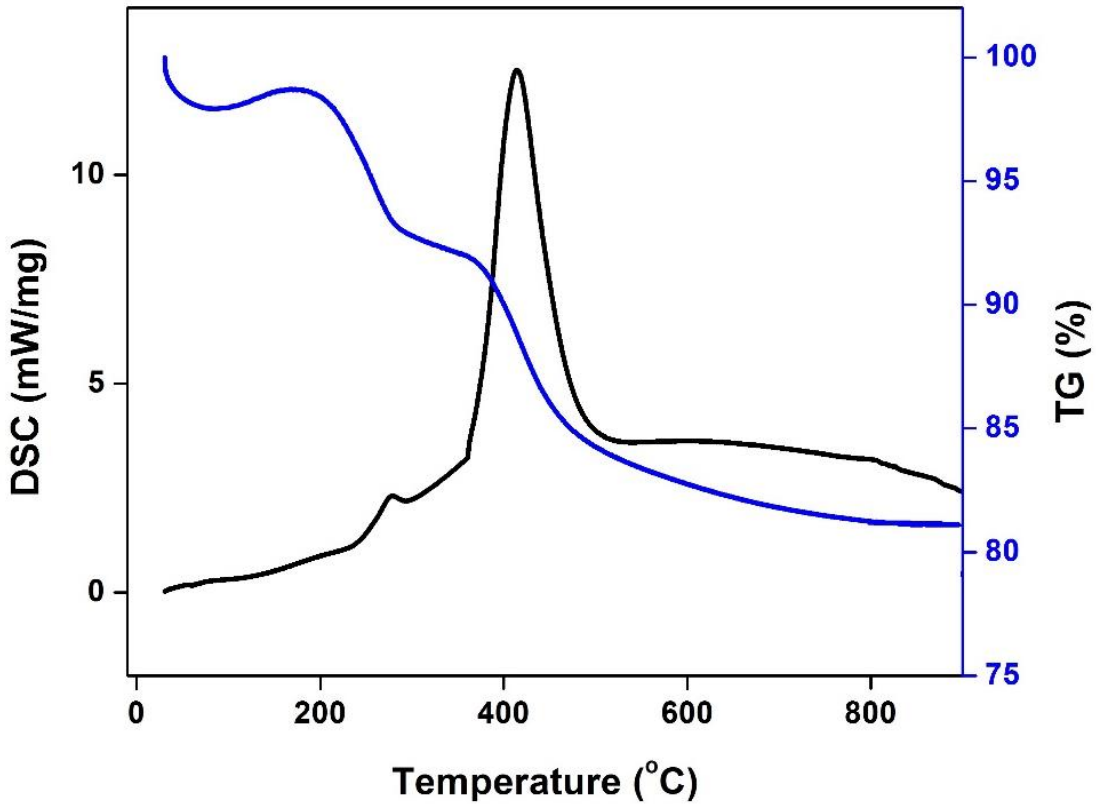

FIG 3.2 DSC TG graph of Polymethylsilsesquioxane

Fig 3.2 shows the simultaneous DSC TG curve of polymethylsilsesquioxane measured upto 850^{o}C under the continuous flow of oxidative atmosphere. From the DSC curve we observed a sharp exothermic peak at 570^{o}C. This peak is observed due to the oxidation of organic matter from the preceramic polymer at this temperature. The weight loss of the polymer takes place in three distinct steps. In the first step (RT-100^{o}C), the weight loss of about 2% takes place which could be due to the removal of adsorbed water. A small exothermic peak around 275^{o}C is observed which is accompanied by a further weight loss of around 6% in the second step (100- 300^{o}C) of TG curve. The weight loss could be attributed to the initial conversion of $CH_3SiO_{1.5}$ to SiO_2 although the amount of conversion to SiO_2 is small. [20]. The third step of the weight loss (300- 800^{o}C) in TG curve is about 10% (above 300^{o}C). This weight loss is due to complete decomposition of the methylsilsesquioxane to silica. A sharp exothermic peak centred at 412^{o}C was observed in the DSC curve which explains the weight loss in the TG curve, and the accompanied crystallisation of SiO_2 from the polymeric precursors.

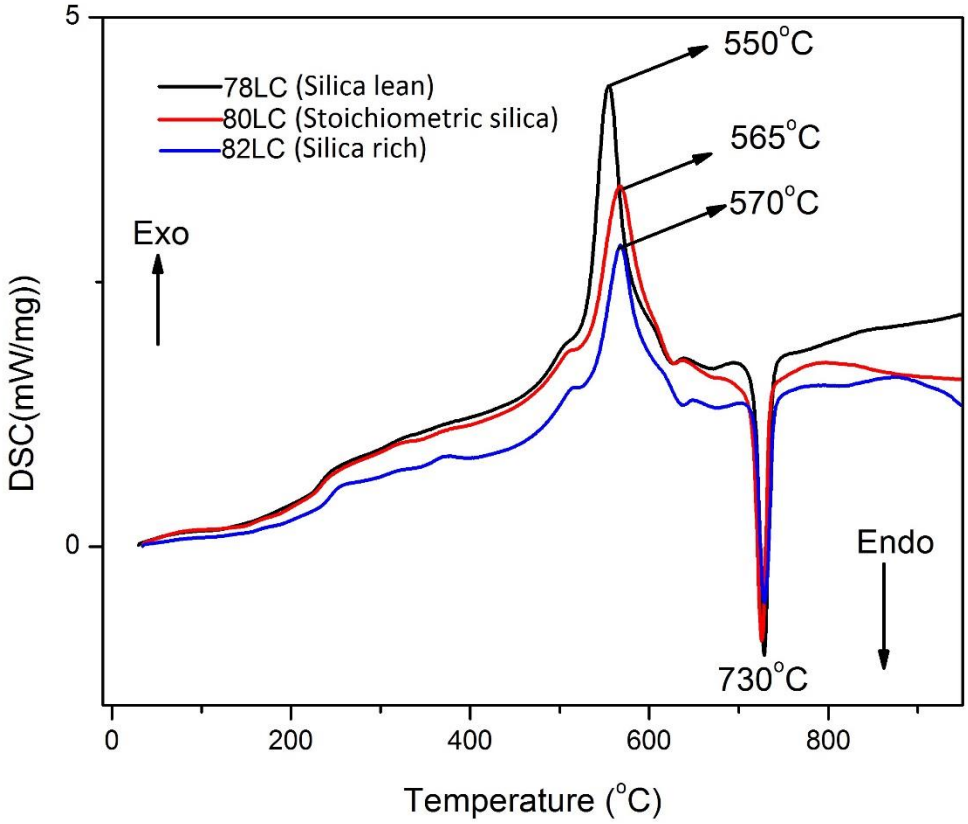

FIG 3.3 DSC graph of 78LC, 80LC and 82LC

Fig 3.2 shows the DSC curve of uncalcined powders prepared with different compositions labelled as 78LC, 80LC and 82LC respectively upto 950^{o}C under a flowing oxidative atmosphere. In all the three DSC curve in figure 3.3 we observed one sharp exothermic peak around 550^{o}C-570^{o}C and another sharp endothermic peak at 730^{o}C. The first peak (between 550^{o}c-570^{o}c) is interesting as it is different from the SiO_2 crystallisation peak from the preceramic polymer at almost 400^{o}c.It appears that the crystallisation of Li_4SiO_4 phase starts to occur in this temperature range. It could be observed that (from table 3.1) with the decrease in the actual amount of silica in 78LC, 80LC and 82LC batches, the exothermicity decreases slightly with the peak position shifting to higher temperatures. This is an interesting find that the mixture having marginally higher amount of polymeric precursor (thus SiO_2) has more reactivity and is kinetically favourable with with early

formation of Li_4SiO_4 phase. A sharp endothermic peak is observed in each curve which is due to the decomposition of lithium carbonate as confirmed from the DSC curve of fig 3.1. It follows that although Li_4SiO_4 formation starts as early as 550^{o}c some of the unreacted Li_2CO_3 decomposes at a later stage i.e at 730^{o}C.

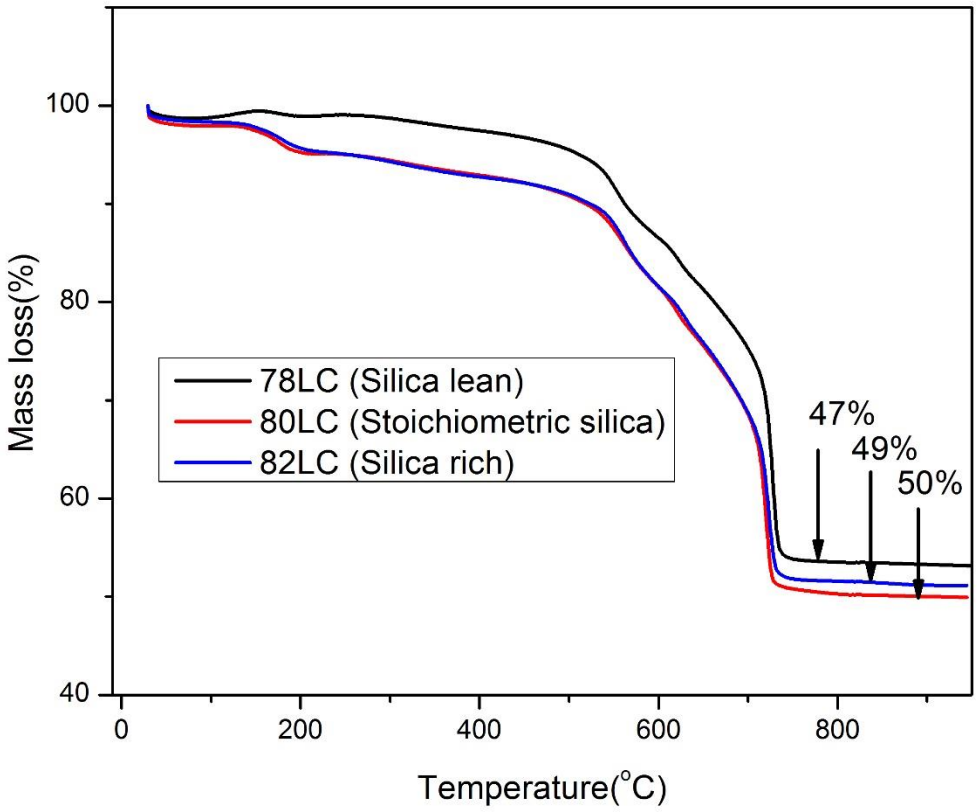

FIG 3.4 TG graph of 78LC, 80LC and 82LC

Fig 3.4 shows the TG curve of uncalcined powders prepared with different compositions labelled as 78LC, 80LC and 82LC respectively upto 950^{o}C under the continuous flow of oxidative atmosphere. It could be observed that overall weight loss of 47%,49% and 50% took place for 78LC, 80LC and 82LC samples respectively.

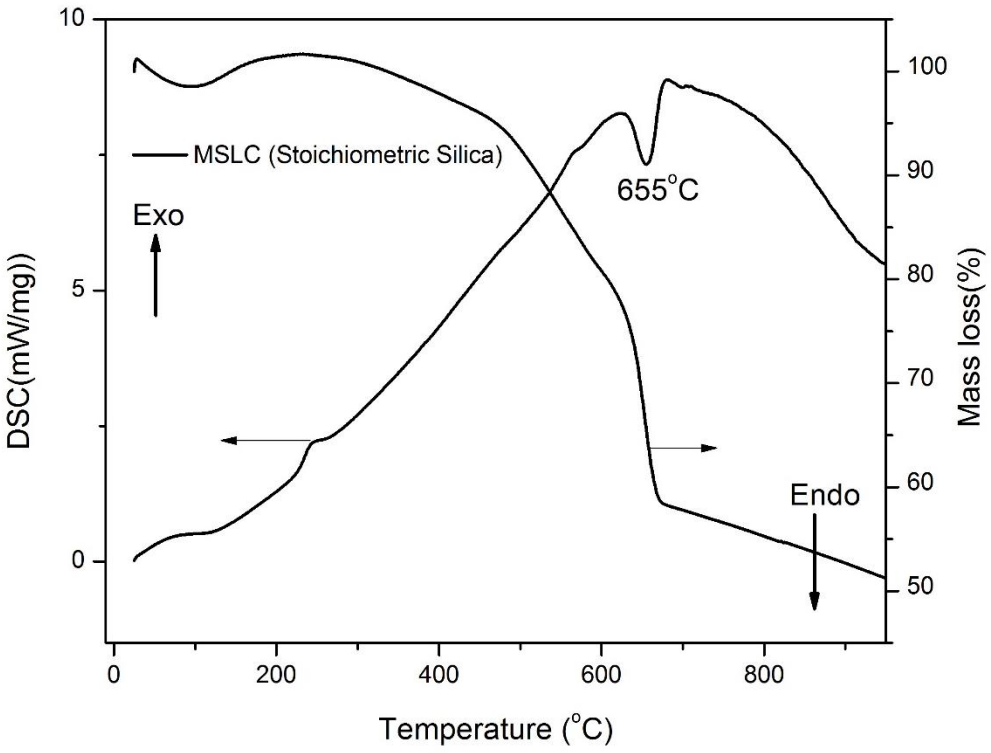

FIG 3.5 DSC TG graph of MSLC

Fig 3.5 shows the simultaneous DSC-TG curve of uncalcined powders prepared with microfine silica and lithium carbonate. The DSC curve showed one small exothermic peak and another sharp endothermic peak at 275^{o}C and 655^{o}C respectively. An overall weight loss of about ~48% occurs which is accompanied by the presence of endothermic peak. The weight loss after 500^{o}C is attributed to the initial decomposition of lithium carbonate and simultaneous reaction of lithium carbonate and microfine silica to form lithium orthosilicate.

3.3 XRD Analysis of the calcined powders

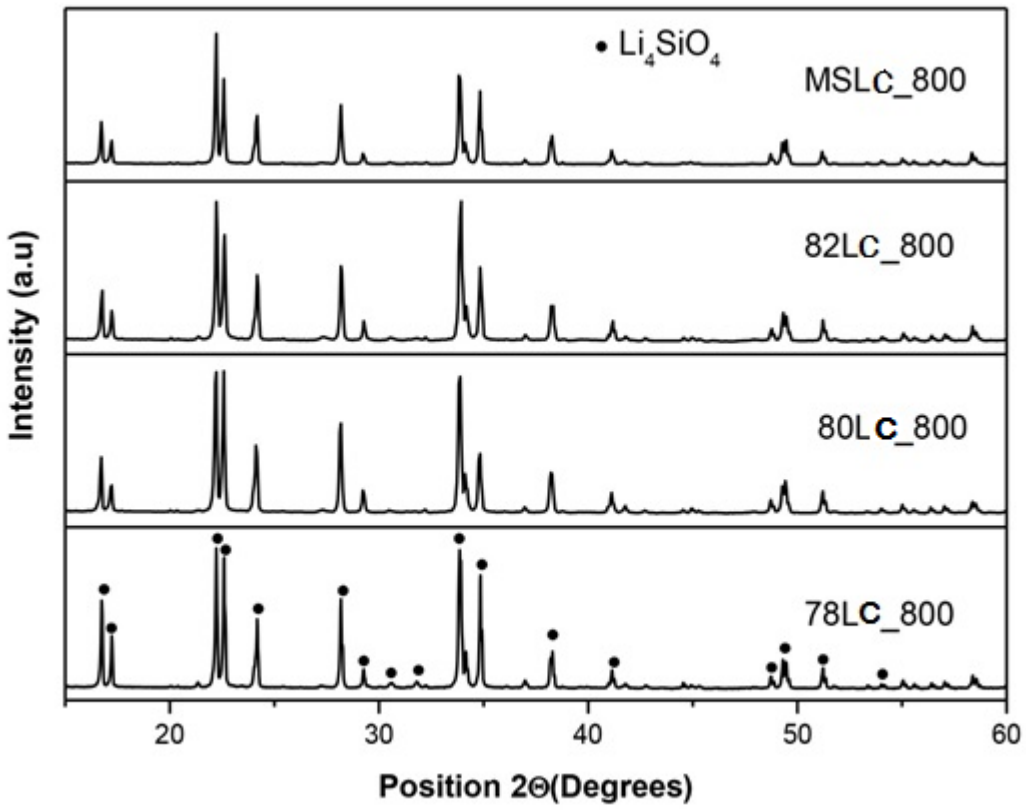

FIG 3.6 XRD GRAPH for 78LC, 80LC, 82LC and MSLC samples calcined at 800^{o}C

Fig 3.6 showed the XRD graph for 78LC, 80LC, 82LC and MSLC samples calcined at 800^{o}C with a dwelling time of 4hrs. Calcination temperature of 800^{o}C was chosen based on the literature reports published elsewhere [17]. All the XRD patterns were scanned from 2θ position in the range of 15^o-60^o.It was observed form the XRD graph that Li_4SiO_4 was the major phase present for all the four samples. The Li_4SiO_4 phase was confirmed from the standard file with reference code 37-1472. It was found that the obtained structure was monoclinic with space group p21/mm.

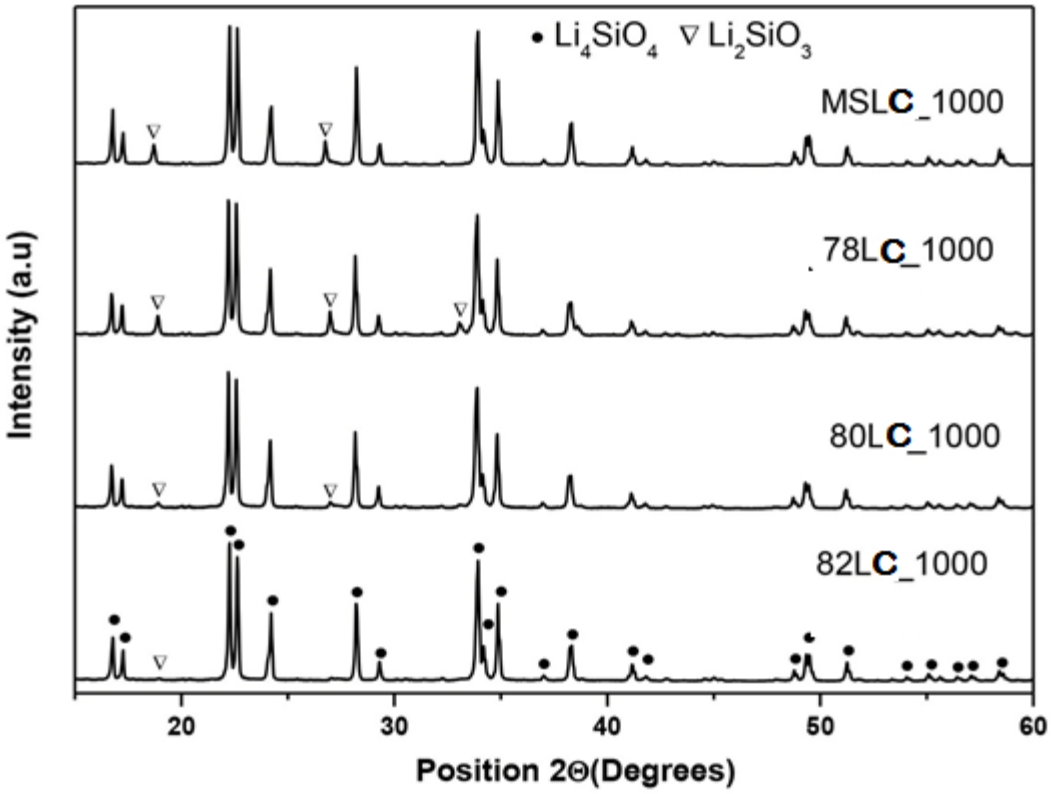

FIG 3.7 XRD Graph for 78LC, 80LC, 82LC and MSLC samples calcined at 1000^0c

Figure 3.7 shows the XRD graph for 78LC, 80LC, 82LC and MSLC sintered samples at 1000^{o}C dwelling time of 4 hours. All the XRD patterns represents patterns with 2θ position in the range of 15^o- 60^o. The 78LC sample clearly showed the phase stability of Li_4SiO_4 phase even after high temperature calcination. The 80LC sample also had similar features. However only a very subtle and faint set of peaks appear that exhibit nucleation of the lithium metasilicate phase. The 82LC sample as well as the MSLC samples exhibited clear formation of the metasilicate phase. Therefore it is observed that a slightly increased amount of SiO_2 results in the stoichiometric formation of Li_3SiO_3. The original stoichiometric composition (82LC) shows slight formation of metasilicate phase formation. This could be explained by the evaporation of Li during heat treatment.

.

3.4 Microstructural Analysis of the sintered specimens

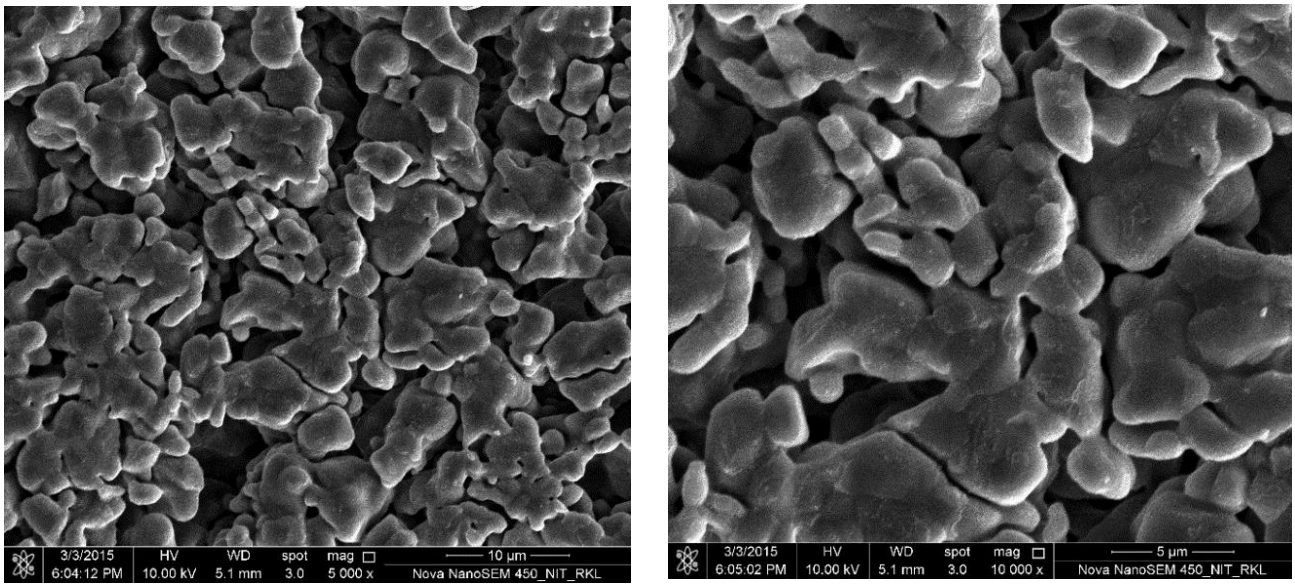

(a) (b)

Fig 3.8: FESEM pictures of MSLC samples sintered at 900^{o}C/4 hours

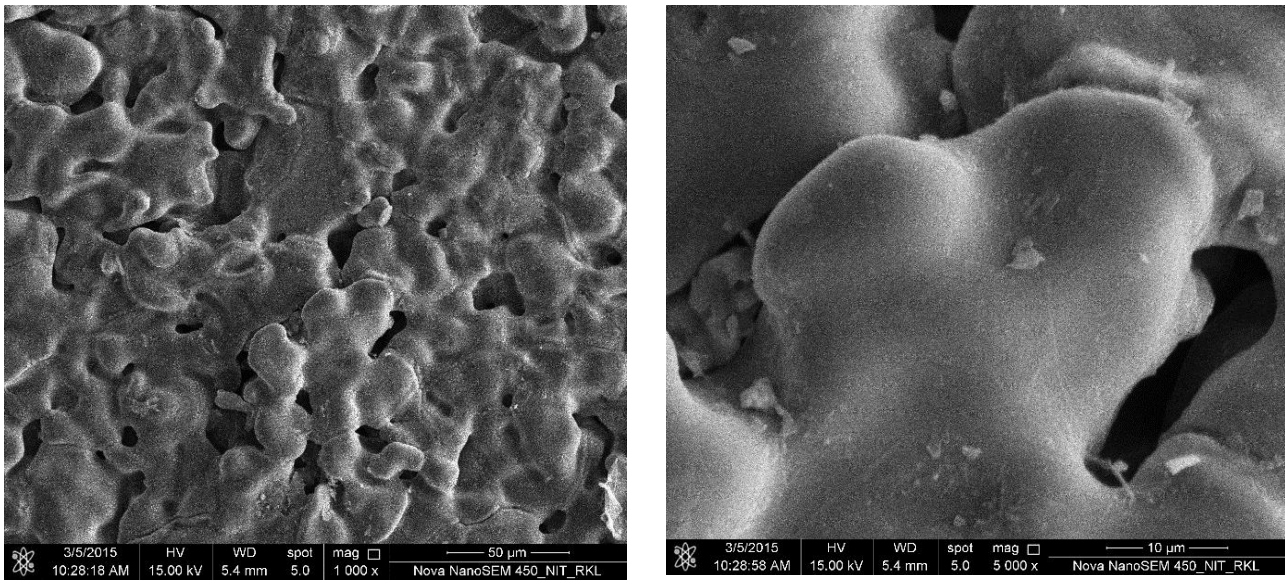

(a) (b)

Fig 3.9: FESEM pictures of 78LC samples sintered at 900^{o}C/4 hours

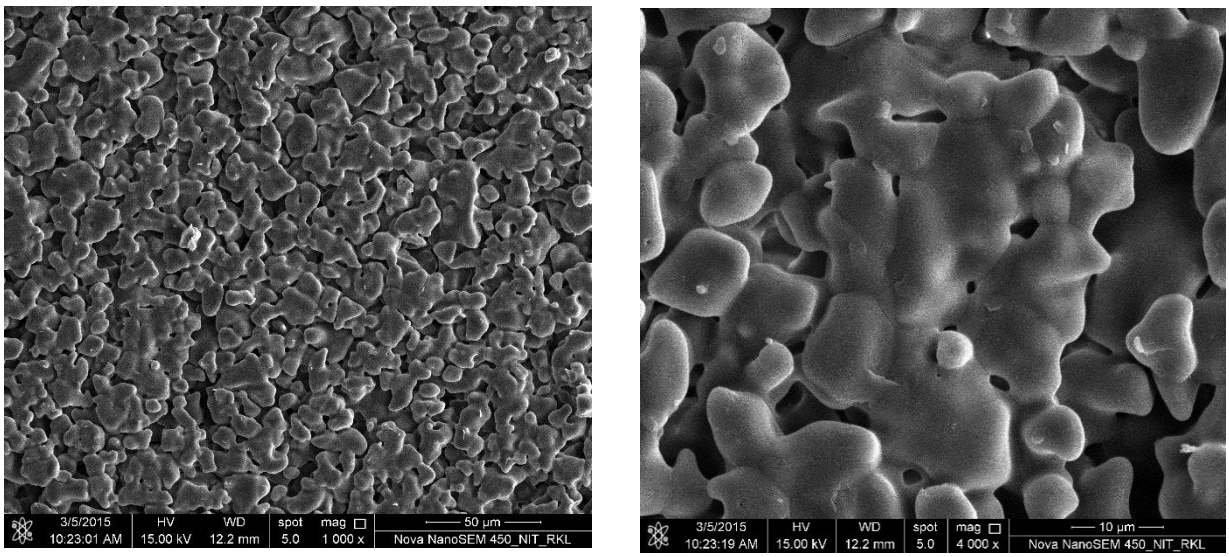

(a) (b)

Fig 3.10: FESEM pictures of 80LC samples sintered at 900^{o}C/4 hours

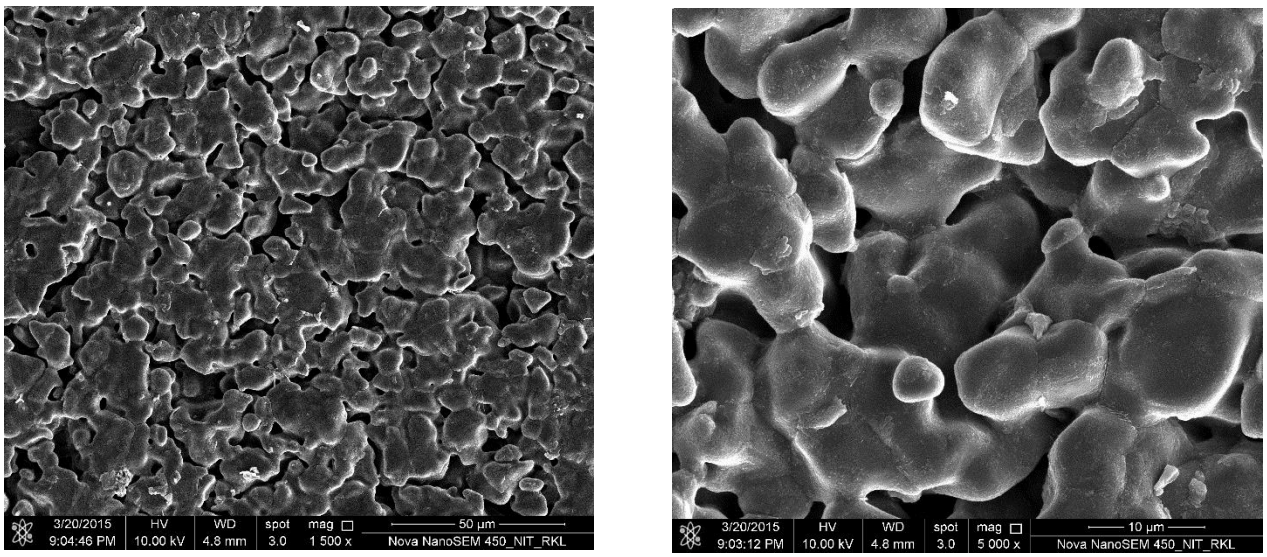

(a) (b)

Fig 3.11: FESEM pictures of 82LC samples sintered at 900^{o}C/4 hours

From Fig 3.8, Fig 3.9, Fig 3.10 and Fig 3.11 we can observe that there is increase in density with decrease in the polymer(methylsilsesquioxane) content for samples sintered at 900^{o}C/4 hours. As can be seen from Fig 3.8 78LC is the most porous followed by 80LC and 82LC. No metasilicate

phases can be observed in any of the samples. Smallest grain (>10 µm) size was observed in MSLC samples sintered at 900ºC.

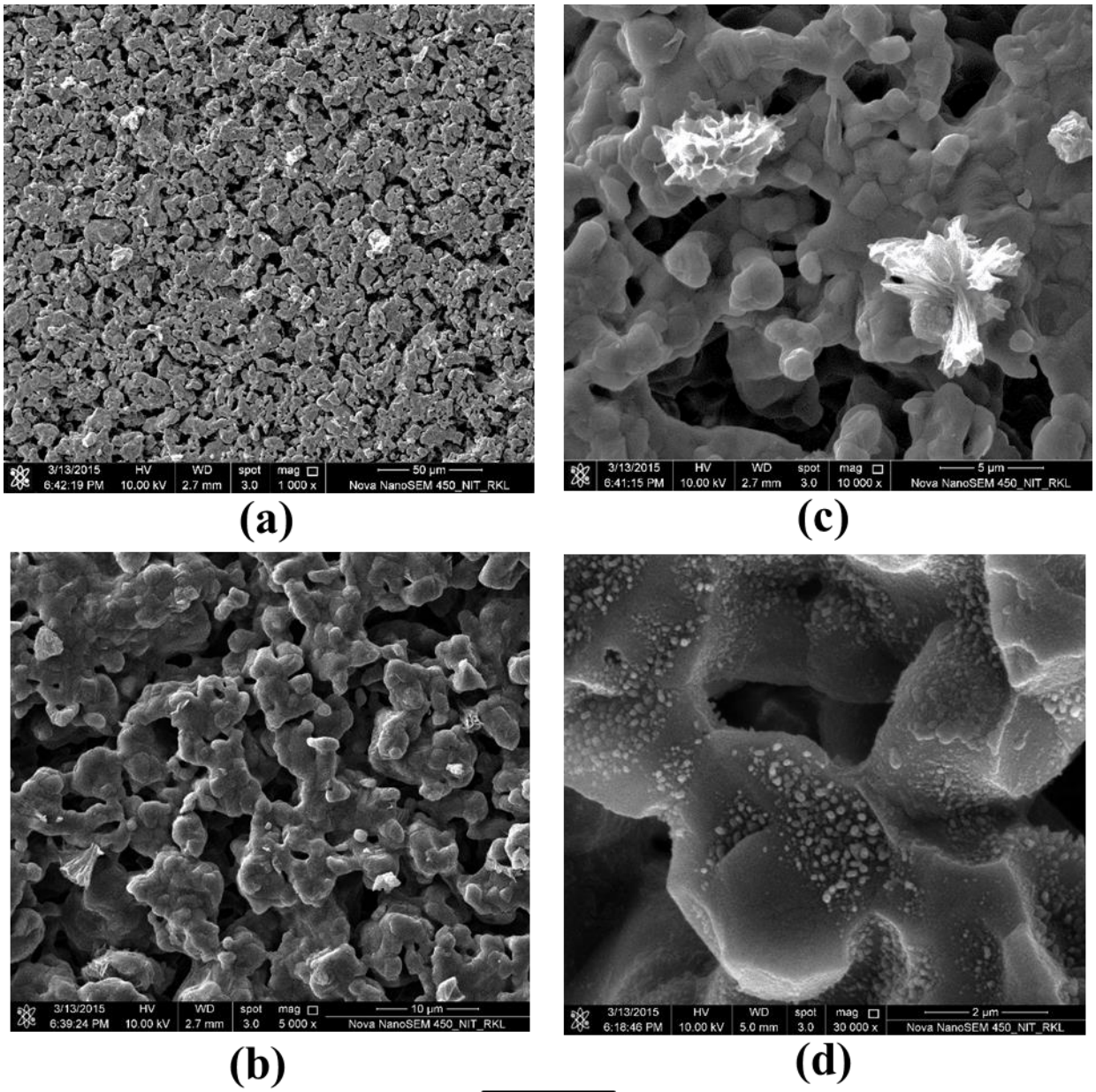

Fig 3.12 FESEM pictures of MSLC pellets sintered at 1000ºC/4hrs with different magnification (a-d)

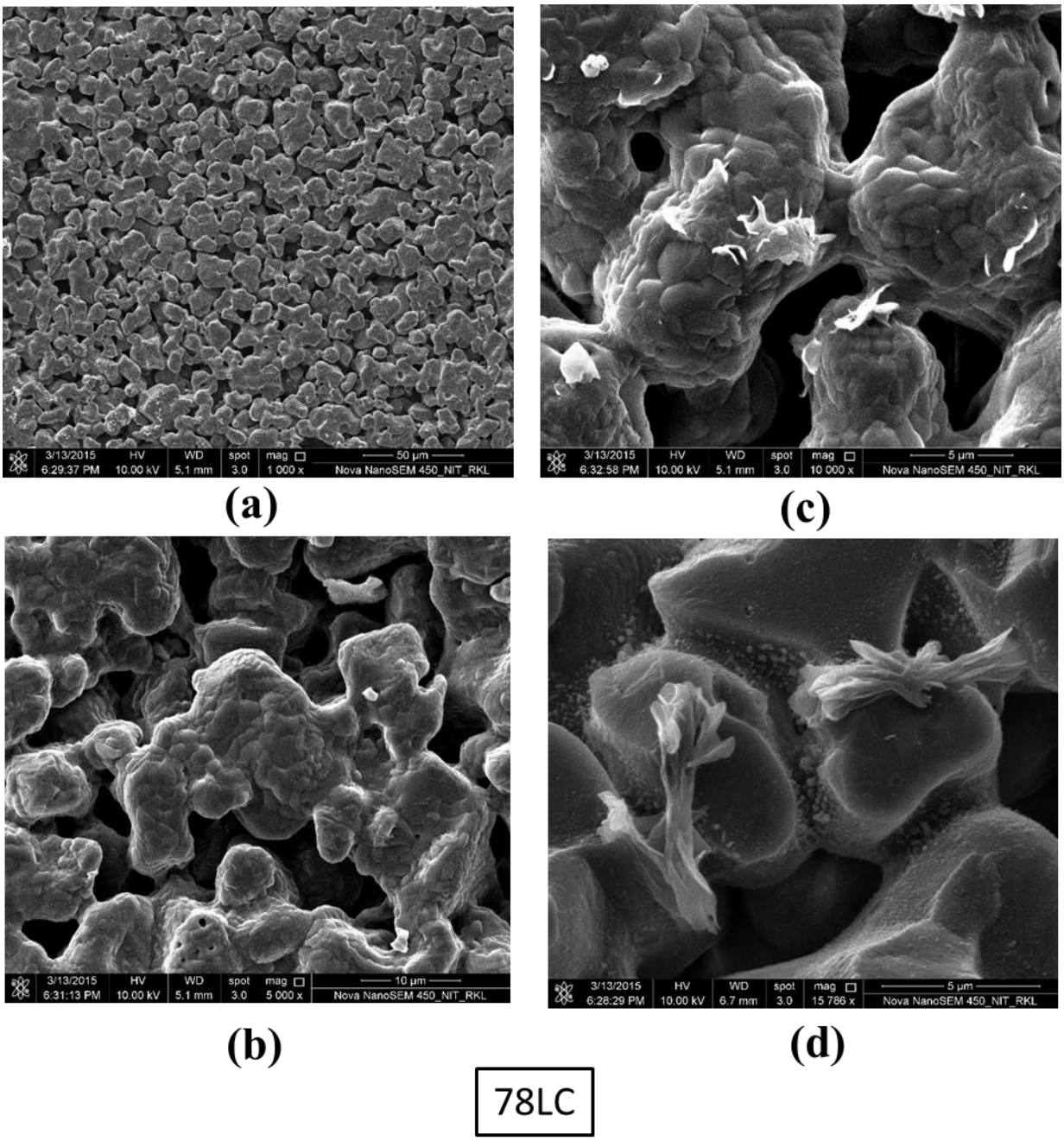

Fig 3.13 FESEM pictures of 78LC pellets sintered at 1000^{o}C/4hrs with different magnification (a-d)

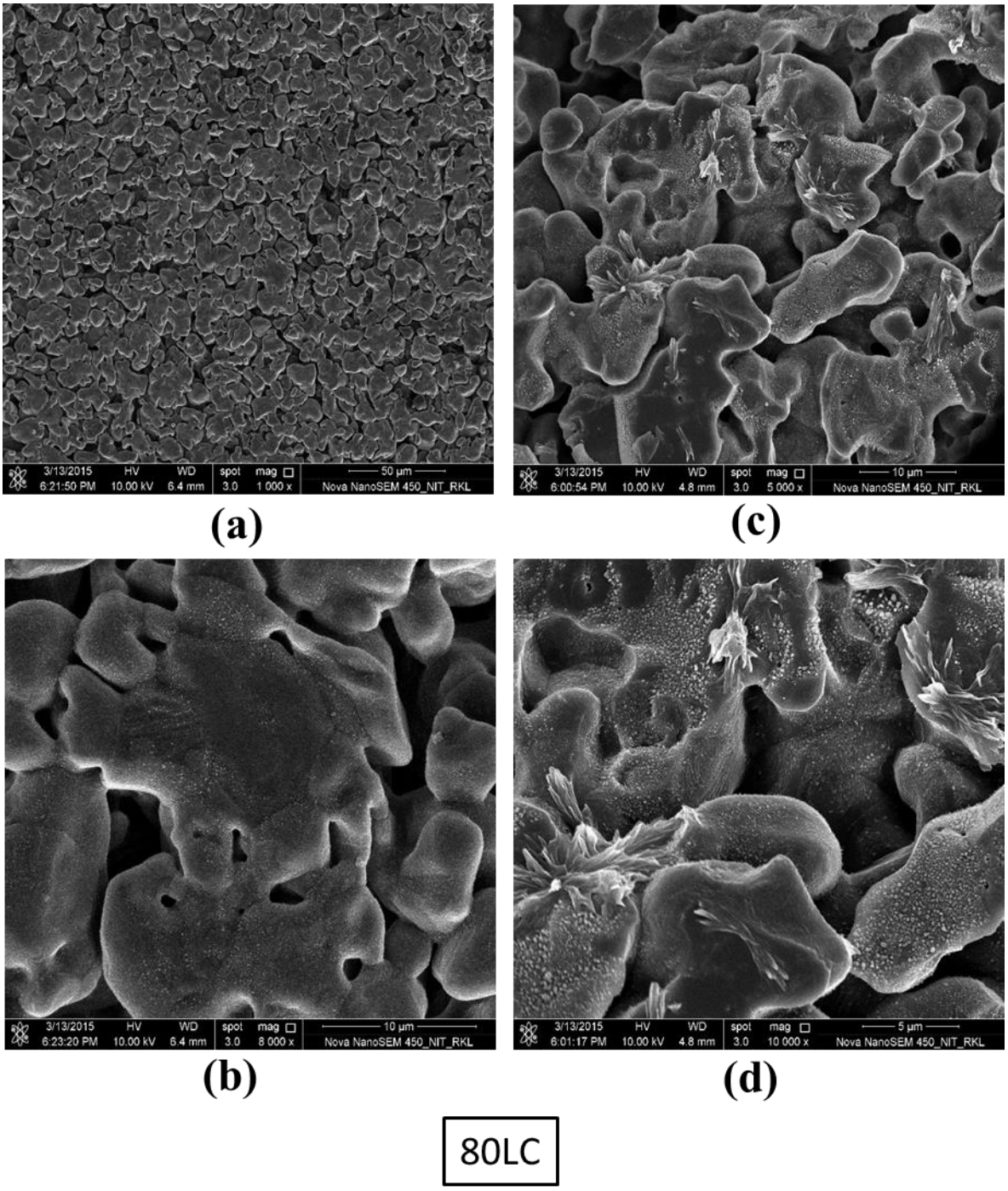

Fig 3.14 FESEM pictures of 80LC pellets sintered at 1000^{o}C/4hrs with different magnification (a-d)

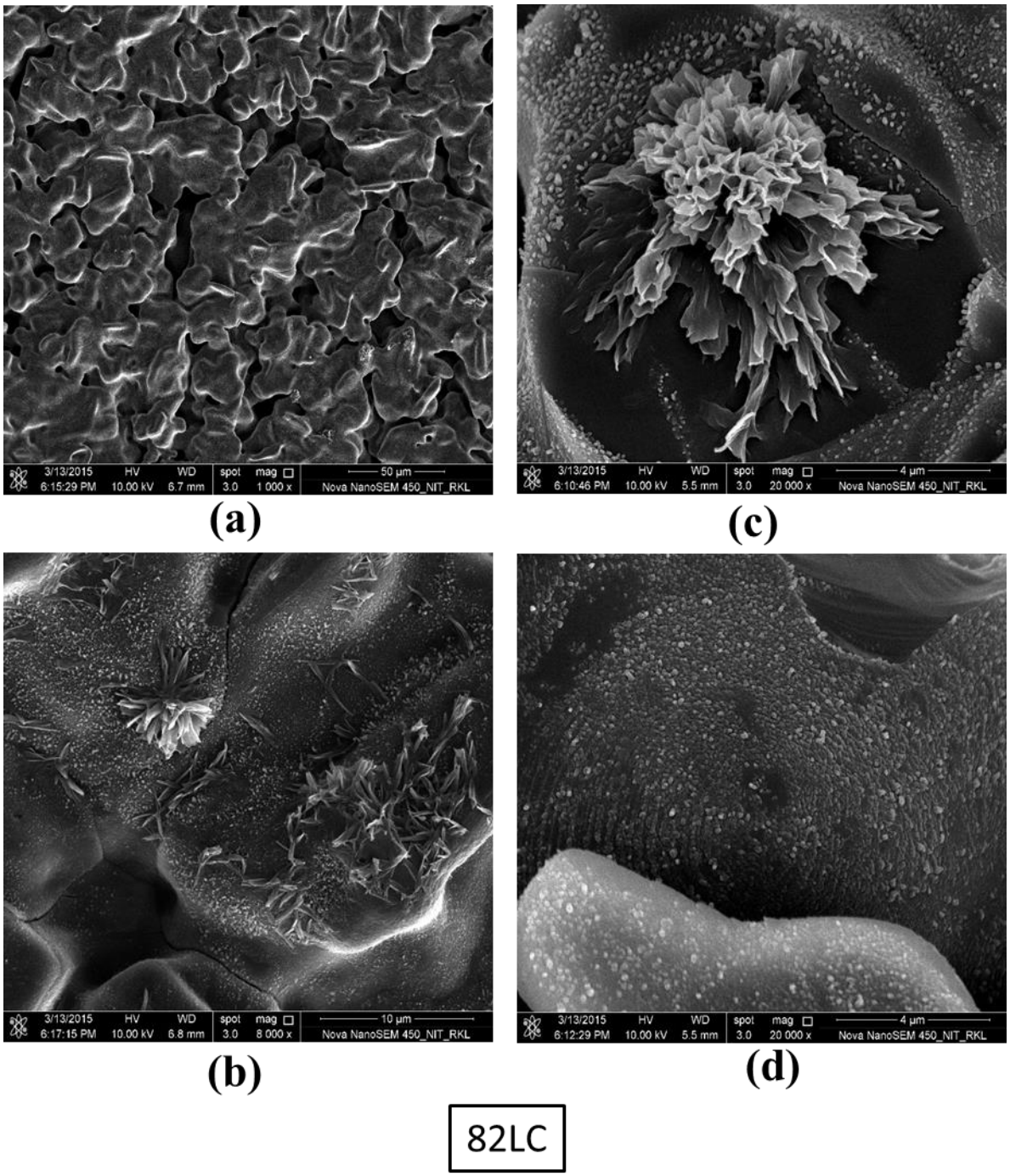

Fig 3.15 FESEM pictures of 82LC pellets sintered at 1000^{o}C/4hrs with different magnification (a-d)

From Fig 3.12, Fig 3.13, Fig 3.14 and Fig 3.15 we can see needle shaped structures in all the four samples sintered at 1000^{o}C/4hrs. These needle shaped structures could be lithium metasilicate phase. Lithium metasilicate phase is formed due to lithium loss at 1000^{o}C from lithium

orthosilicate. The sublimation of Lithium around 1000°C can be confirmed from the phase diagram as shown in figure 3.18. The presence of needle shaped structures creates voids in the specimens which reduces the densification process. One could also observe that MSLC sample showed very few needle shaped structures which shows that lithium evaporation is minimum

3.5 Bulk Density and Apparent Porosity measurement of sintered samples

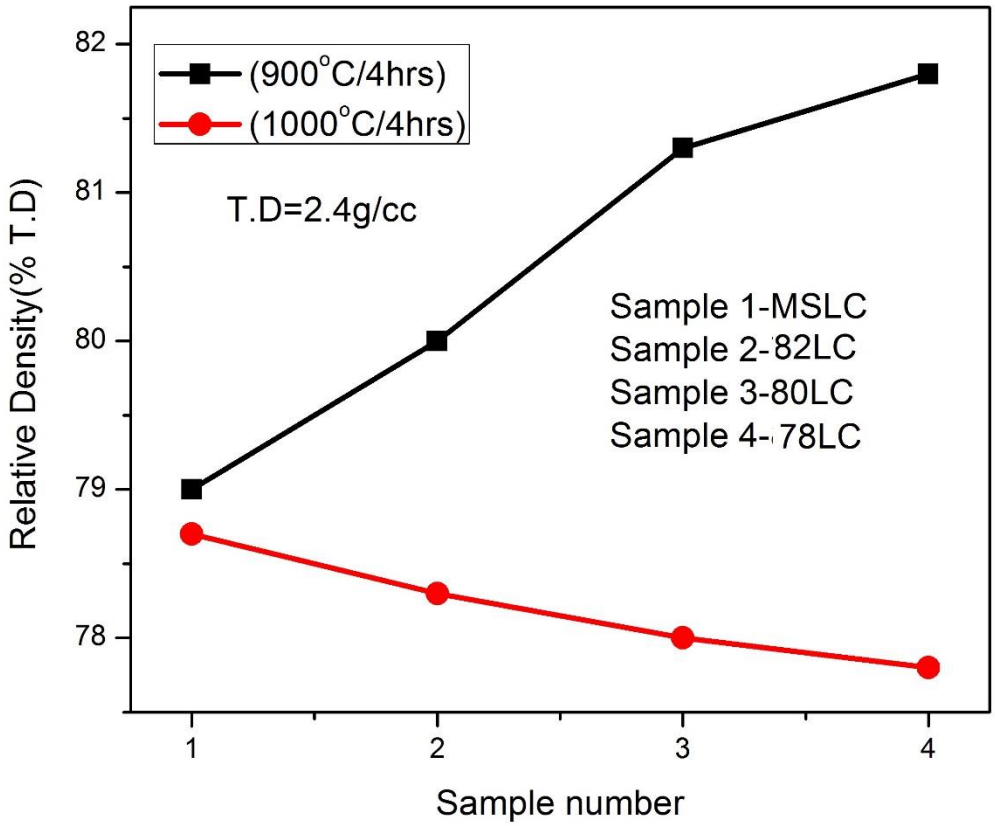

Fig 3.16 Relative density for MSLC, 78LC, 80LC and 82LC samples sintered at 900°C and 1000°C/4hrs

Figure 3.16 shows the graph between relative density (function of Theoretical Density) vs different samples sintered at 900°C and 1000°C. It could be observed that the relative density increased with the increase in content of polymethylsilsesquioxane when the pellets were sintered at 900°C/4hrs. However, the trend in the relative density values for all samples sintered at 1000°C/4hrs is different than samples sintered at 900°C/4hrs. The possible reasons for such a decrease in the density values at 1000°C has been explained in the section 3.4.

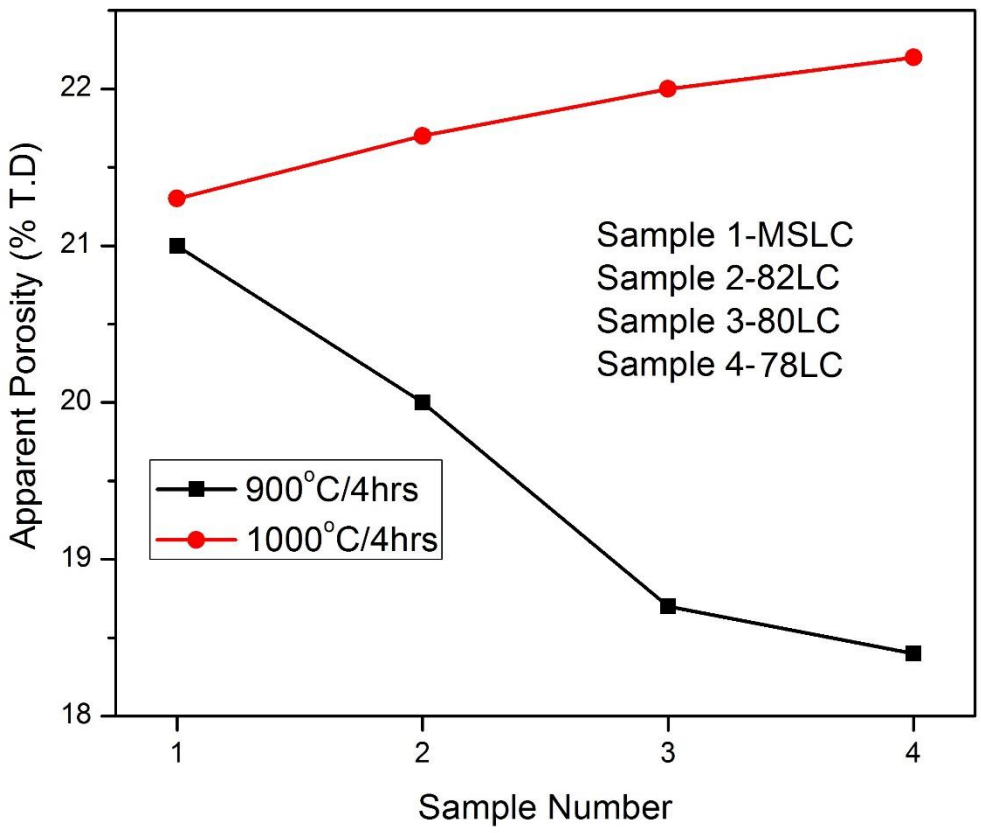

Fig 3.17 Apparent porosity for MSLC, 78LC, 80LC and 82LC samples sintered at 900°C and 1000°C/4hrs

Figure 3.17 showed the graph between apparent porosity for different samples sintered at 900°C/4hrs and 1000°C/4hrs. It was observed that apparent porosity increased from sample 1 to sample number 4 when sintered at 1000°C/4hrs. This increase in porosity is explained by the formation of more pores in the samples created due to the evaporation of lithium oxide. For 900°C sintered samples the porosity is decreased from sample 1 to sample number 4.

Possible reasons for the decrease in density

a) Presence of lithium metasilicate phase above 1000^{o}C

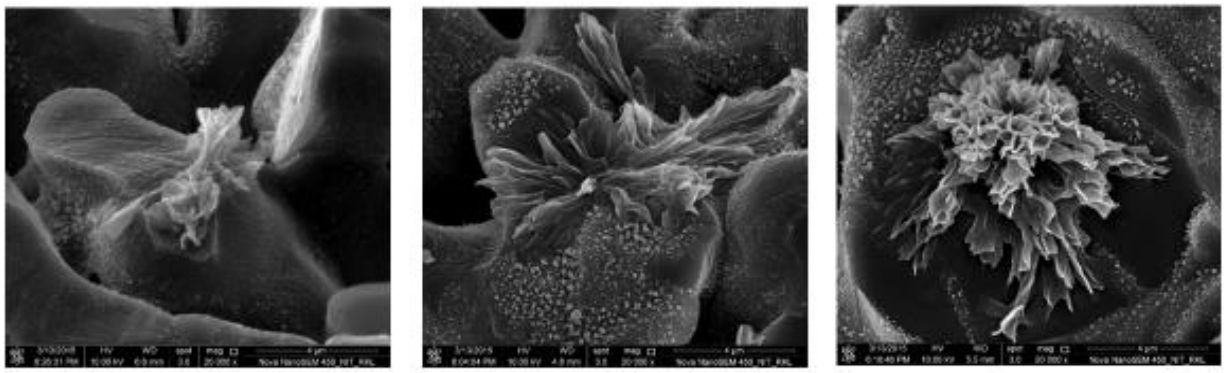

Fig 3.18 FESEM pictures of 78LC, 80LC and 82LC pellets sintered at 1000^{o}C/4hrs

From the above graph we could see that there are no needle shaped structures at 900 ^{o}C because of the absence of lithium metasilicate phase but at 1000^{o}C we could see needle shaped structures in all the three batches of 78%, 80% and 82% silica yield. These structures may be lithium metasilicate. This metasilicate phase formation takes place due to lithium loss at high temperature.

b) Phase diagram of Li_2O-SiO_2 system

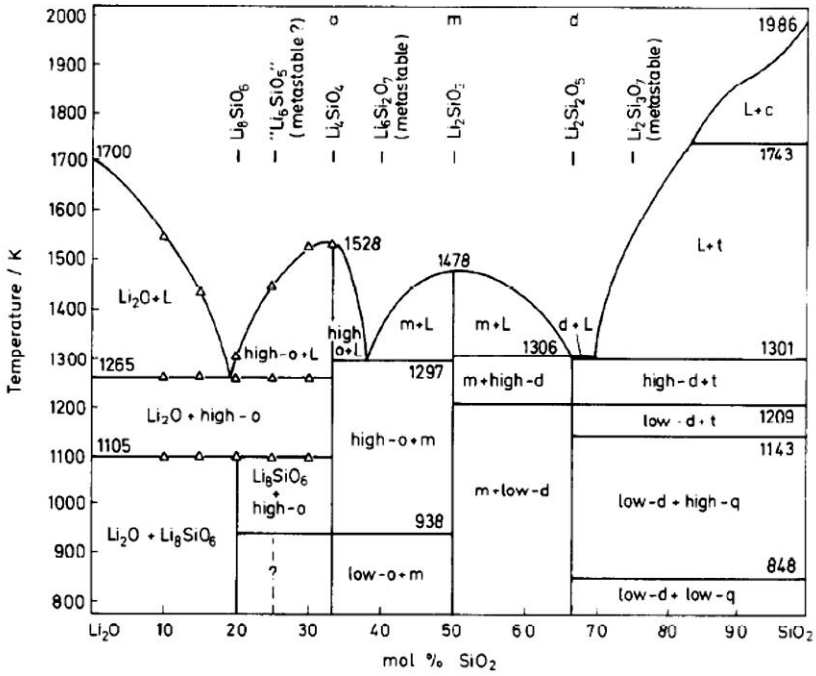

Fig 3.18The phase diagram of the Li_2O-SiO_2 system according to ref. [21]

The intermediate position of Lithium between those of alkalis and the alkaline earths is evidenced in the nature of the compounds formed and in their properties. The choice of taking different amounts of polymer arise from the phase diagram. We could observe that at higher temperature (above 1000^{o}C) there is the formation of lithium metasilicate phase. Thus to reduce the sublimation of lithium oxide and formation of metasilicate phase we look out at the possibility of minimising the lithium loss by going for silica rich and silica lean batches.

CHAPTER 4
CONCLUSION

The work embodied in this dissertation can be summarized as follows:

- Phase pure lithium orthosilicate powder was prepared from a polymer derived ceramics approach at 800^{o}C.
- The properties of lithium orthosilicate derived using two different sources of silica were compared.
- XRD analysis confirmed that phase pure lithium orthosilicate can be obtained for all the four batches i.e MSLC, 78LC, 80LC and 82LC after calcining at 800^{o}C.
- With increase in the sintering temperature from 900 ^{o}C to 1000 ^{o}C we could observe minute formation of lithium metasilicate peaks. This concludes that lithium orthosilicate remain stable and can only be used below 1000 ^{o}C for targeted applications.
- At 1000^{O}c the formation of Li_3SiO_3 was clearly observed for microfine silica based batch as well as the silsequixone based as well as the batch that had lower SiO_2 content.
- Stoichiometric batch (80LC) as well as SiO_2 lean batch (82LC) exhibited only subtle formation of metasilicate phase. This could be attributed to the dynamic composition of the system due to lithium loss. The containing lower SiO_2 (82LC) yielded better stoichiometric Li_4SiO_4 due to loss of Lithium thus adjusting the composition to stoichiometry.
- From the FESEM analysis it could also be observed that all samples sintered at 1000 ^{o}C showed needle or spike like structures which could be lithium metasilicate.It can be concluded that changing the silica amount can reduce/increase the formation of lithium metasilicate but cannot completely eliminate it.
- 78LC samples showed highest density when sintered at 900^{o}C/4hrs which shows that difference in amount of silica affects the densification process. Also 78LC samples showed lowest density when sintered at 1000^{o}C/4hrs which can be attributed to the formation of lithium metasilicate phase that can be confirmed from fig 3.7(xrd graph)

Reference

[1] R. F. Speyer, Thermal Analysis of materials, 2 nd ed ,Mercel Dekker, (1993) 35-46.

[2] D. Cruz, S. Bulbulian, E. Lima, and H. Pfeiffer, J. Solid State Chem.179 {3}(2006) 909.

[3] G. Mondragon-Gutierrez,D. Cruz,H. Pfeiffer, S.Bulbulian,Res. Lett. Mater. SciArticle ID 908654 (2008)

[4] B.N. Nair, R.P. Burwood, V.J. Goh, K. Nakagawa, T. Yamaguchi, Progress in Materials Science 54 (2009) 511–541.

[5] B. Banov, J. Bourilkov, M. Mladenov, J. Power Sources 54 (1995)

[6] A.G. Ritchie, C.O. Giwa, J.C. Lee, P. Bowles, A. Gilmour, J. Allan, D.A. Rice, F. Brady, S.C.E. Tsang, J. Power Sources 80 (1999) 98

[7] Lu-Lu Zhang, Song Duan , Xue-Lin Yang , Gan Liang , Yun-Hui Huang , Xing-Zhong Cao , Jing Yang , Ming Li , Mark C. Croft , Cale Lewis, J. Power Sources 274 (2015) 194-202

[8] B. LiYing , G. Wei1 , SU Yue Feng, W. Zhao , L. Ning , C. Shi & W. Feng, Review on Chinese Science bulletein, (2013) 58{6} 575–584]

[9] D. Vollath, H. Wedemeyer, E. Gunther and H. Elbel, Fusion Eng.Des.8 (1989) 415

[10] D. Vollath, H. Wedemeyer and E. Gunther,J.Nucl.Mater.,133&134 (1985) 221

[11] D. Vollath,H. Wedemeyer,J. Nucl. Mater.141-143 (1986) 334

[12] A.A. Kaukis, J.E. Tiliks, V.V. Tamuzhs, A.A. Abramenkovs, G.K. Kizane, J.A. Ubele V.G. Vasiljev, Fusion Eng. and Des. 17 (1991) 13

[13] Tao Tang, Zhi Zhang, Jian-Bo Meng, De-Li Luo,Fusion Eng. Des. 84 (12) (2009) 2124

[14] D. Cruz and S. Bulbulian, J. Am. Ceram. Soc.88 [7](2005) 1720.

[15] H. Pfeifer, P. Bosch, S. Bulbulian,J. Nucl. Mater 257(1998) 309.

[16] C.C. Chang, C.C. Wang, P.N. Kumta , Mater. Des.22 (2001) 617

[17] X. Wu, Z. Wen, X. Xu, X. Wang, J. Lin, J. Nucl. Mater.392 (2009) 471

[18] A. Choudhary, B.S. Sahu, R. Mazumder, S. Bhattacharyya, P. Chaudhuri, J. Alloys. Comp. 590 (2014) 440–445

[19] P. Colombo, G. Mera and R. Riedel, G. D. Soraru, J. Am. Ceram. Soc.,93[7] 1805–1837 (2010)

[20] A. N. Timoshevskii, M. G. Ktalkherman, V. A. Emelkin, B. A. Pozdnyakova, and A. P. Zamyatin, High Temperature, 2008, Vol. 46, No. 3, pp. 414–421

[21] R. H. Baney, M. Itoh, A. Sakakibara, and T. Suzuk, Chem. Rev. 1995, 95, 1409-1430

[22] F. C. Kracek, J. Phys. Chem. 34 {12} (1930) 2641